RAL-93-103

Science and Engineering Research Council
**Rutherford Appleton Laboratory**
Chilton DIDCOT Oxon OX11 0QX

RAL-93-103

HEP

# Baryogenesis from a Primordial Lepton Asymmetry

**S A Abel and K E C Benson**

December 1993

RAL-93-103

# Baryogenesis from a Primordial Lepton Asymmetry

S. A. Abel[1] and K. E. C. Benson[2]

[1]Rutherford Appleton Laboratory
Chilton, Didcot
Oxon OX11 0QX
England

[2]Theoretical Physics Department
Keble Road
Oxford OX1 3NP
England

December 21, 1993

**Abstract**

We examine the generation of baryon asymmetry at the weak scale from a primordial lepton asymmetry. If the electroweak phase transition is first order, partial reflection of tau leptons off the bubble walls and the resulting hypercharge transport into the symmetric phase, gives rise to a baryon number consistent with observation.

# Introduction

Electroweak theory contains the means for anomalous violation of fermion number via non-perturbative effects, in the form of instantons at zero temperature [1] and sphalerons at high temperature [2]. The vacuum structure of electroweak theory admits both quantum and thermal tunneling between inequivalent vacua by such configurations. Because of this, any theory in which $B - L = 0$ is in danger of having its baryon number erased by sphalerons.

One way around this problem is to suppose that the baryon asymmetry was made at the electroweak scale [3,4]. If this is the case the sphaleron transitions must have fallen out of equilibrium whilst there was still some chemical potential for non-zero baryon number. If the CP violation is provided by the higgs sector, this implies that the phase transition was at least mildly first order [5,6].

The alternative possibility which will concern us here, is that the asymmetry was encoded in a conserved global quantum number such as $B - L$ number [7]. This was generated (or set by hand) primordially, and after possible processing at the electroweak phase transition, was converted into the presently observed baryon number. Recent work [8,9] has suggested that the three

$$L_i - B/3$$

numbers may play this role ($i$ is a generation index). These could have been produced by generational (and CP violating) differences in the out of equilibrium decays of lepto-quarks [8,10]. The baryogenesis could have occurred *after* the electro-weak phase transition as a results of mass effects. For this to be possible it is necessary that sphalerons remained in equilibrium for some time implying a second–order transition. Campbell, Davidson, Ellis, and Olive [11] have taken this idea further by demonstrating how to avoid the $m^2/T^2$ suppression through lepton-violating interactions. Provided that some, but not all, lepton flavours are violated by $\Delta L \neq 0$ interactions in equilibrium, $B$ may be regenerated without the $m^2/T^2$ lepton mass effects. Instead $B$ depends only on the initial asymmetry of the non-equilibrating modes. For example, if lepton-violating interactions equilibrate $L_1 - B/3$ and $L_2 - B/3$ to zero, then the non-zero $L_3 - B/3$ biases baryon production via sphalerons:

$$B \propto B - L = B/3 - L_3 \neq 0 \ .$$

The above example is interesting for two reasons. Firstly it can operate even if $B - L = 0$. Secondly there is the novelty that two of the Sakharov conditions (C/CP violation and thermal non-equilibrium) are important at early times, whilst the third (baryon number violation) is important at 'late' times (where 'late' means at the weak scale; after $\approx 10^{-10}$ seconds). In the light of this, we shall discuss an alternative way in which these quantum numbers can furnish a net baryon number.

Again we rely on some unspecified mechanism to generate a non-zero $L_3 - B/3$ number. The values of the other two numbers are unimportant, and it could be that $B - L = 0$. The phase transition is assumed to be robustly first order, as argued for in the case of the Standard Model in refs.[6,12], and as demonstrated in extensions of it in ref.[13]. Once the temperature drops below the critical temperature, bubbles of true vacuum begin to nucleate and expand into the symmetric phase. As the walls advance through the plasma, a fraction (proportional to their physical mass) of the $\tau$-leptons are reflected back into the symmetric phase. Since the $L_3 - B/3$ number is non-zero, more taus than anti-taus are reflected, and a small hypercharge builds up on the outside of the bubbles with an opposing hypercharge on the inside. On the outside sphaleron transitions convert some of the lepton number into baryons, whilst on the inside sphaleron transitions are suppressed by a large exponential factor, resulting in a net number of baryons being produced.

Since the reflection is only suppressed by the factor $M_\tau/T$ one might expect this mechanism to be much more efficient than the equilibrium process described in refs.[8,9]. We shall see that in fact the two mechanisms give remarkably similar baryon asymmetries. This is due to an additional suppression due to the low rate of conversion of lepton into baryon number compared to the typical wall velocity. The resulting baryon number is proportional to the initial $\tau$-lepton asymmetry $\rho_\tau$. We stress that we do not make any assumption about enhanced (or maximal) CP violation in the dynamics of the phase transition (which plays no role in our mechanism [1]).

At high temperature or density, the fundamental excitations do not coincide with the elementary particles. As a result, perturbation theory in terms of the bare fields does not properly describe effects essentially due to the ambient plasma. In order to proceed in a valid perturbative calculation, we first determine the quasiparticle modes that exist in a relativistic plasma at high temperature. Using these modes, we compute the reflection coefficients and then the lepton flux reflected off the expanding bubble wall. Because the reflected flux $\propto M_l/T$, where $M_l$ is the lepton flavour mass and $T \sim 100$ GeV is the critical temperature of the phase transition, the $\tau$-lepton flux will predominate. The thermal scattering length of the leptonic quasiparticles will then be computed, to give an indication of how long the reflected leptons remain in the unbroken phase before being absorbed by the advancing front of broken phase. During its time in the unbroken phase, the $\tau$-lepton flux biases anomalous baryon violation, which, it is assumed, are in equilibrium outside the bubble (the region of $\phi = 0$). The sphaleron processes thus produce baryons, which are swallowed into the broken phase and survive to the present. We then estimate the generated baryon number and find that $\rho_B \sim 10^{-10}$ can be accommodated in this scenario, provided that the primordial $\tau$-asymmetry is $\rho_\tau/s \sim 5\cdot 10^{-5}$, for a wall velocity $u \approx 0.1$. Scaling by the lepton number density,

$$\frac{n_l - n_{\bar{l}}}{n_l + n_{\bar{l}}} \sim 0.005 \; .$$

Our primary sources are the papers by Nelson, Kaplan, and Cohen [4] and by Farrar and Shaposhnikov [12], denoted NKC and FS respectively. The starting point of our

[1]CP violation is of course evident in the initial condition of a primordial L-asymmetry; and CP violation in the particle dynamics would have been required for its generation at the GUT scale, as required by the Sakharov conditions.

analysis is the rate equation describing the approach of baryon number to equilibrium [14];

$$\dot{\rho}_B = -\frac{\Gamma_B}{T}\frac{\partial F}{\partial B} \,. \tag{1}$$

The partial derivative of the free energy is taken with all conserved quantum numbers held fixed, and as we will compute later, is simply proportional to the hypercharge;

$$\frac{\partial F}{\partial B} = \xi \frac{\rho_Y}{T^2} \,, \tag{2}$$

where the parameter $\xi$ depends on the model under consideration and will be determined explicitly later. Integrating the rate equation ahead of the advancing bubble wall,

$$\begin{aligned} \rho_B &= -\frac{\Gamma_B}{T}\int dt \, \frac{\partial F}{\partial B} = -\frac{\xi \Gamma_B}{T^3}\int_{-\infty}^{z/u} dt \, \rho_Y(z-ut) \\ &= -\frac{\xi \Gamma_B f_Y \tau_T}{u T^3} \,, \end{aligned} \tag{3}$$

where $f_Y$ is the reflected hypercharge flux and $\tau_T$ the thermal transport time ($\sim$ thermal scattering length). Scaling by the entropy density and recalling the rate for anomalous baryon violation in the symmetric phase (for three generations) [15,16],

$$\Gamma_B = 3\kappa \alpha_{\mathrm{W}}^4 T^4 \,, \tag{4}$$

we arrive at our final expression for the observed baryon number,

$$\frac{\rho_B}{s} = -\frac{3\alpha_{\mathrm{W}}^4 \kappa \xi}{u}\left(\frac{f_Y \tau_T T}{s}\right) \,. \tag{5}$$

We consider the ranges $0.1 < \kappa < 1$ [16] and $0.1 < u < 1$ [17], and are left to compute $f_Y$, $\xi$, and $\tau_T$, which we do in the following sections. For the remainder of this discussion, we shall assume for concreteness that $B - L = 0$, although this is not necessarily the case as stated previously.

# Reflected Hypercharge flux ($f_Y$)

Before we can calculate $f_Y$ we need to determine the leptonic modes in the thermal plasma (which is characterised by the four-velocity $u^\alpha$) and obtain the quasiparticle solutions for left and right chiralities, which have different interactions and hence develop different thermal masses. The first part of this section section summarises basic results; more complete treatments may be found in Weldon and Lebedev [18].

The lepton thermal self-energy at one loop is given by

$$\begin{aligned} \Sigma(P) &= iA\int \frac{d^4k}{(2\pi)^4}\, D_{\mu\nu}(k)\gamma^\mu S(k+P)\gamma^\nu + iB\int \frac{d^4k}{(2\pi)^4}\, D(k)S(k+P) && (6) \\ &\equiv -a(\omega,p)\, \not{P} - b(\omega,p)\, \not{u} \,, && (7) \end{aligned}$$

where $a$ and $b$ are functions of the Lorentz invariants

$$\begin{aligned} \omega &\equiv P \cdot u && (8) \\ p &\equiv \sqrt{(P \cdot u)^2 - P^2}\,, && (9) \end{aligned}$$

such that $\omega^2 - p^2 = P^2$. The functions $a$ and $b$ are computed in [18]:

$$\begin{aligned} a(\omega,p) &= \frac{\Omega^2}{p^2}\left[1 - \frac{\omega}{2p}\log\left(\frac{\omega+p}{\omega-p}\right)\right] && (10) \\ b(\omega,p) &= \frac{\Omega^2}{p}\left[-\frac{\omega}{p} + \frac{1}{2}\left(\frac{\omega^2}{p^2} - 1\right)\log\left(\frac{\omega+p}{\omega-p}\right)\right] && (11) \\ \Omega^2 &= (A + \frac{1}{2}B)\frac{T^2}{8}\,. && (12) \end{aligned}$$

The constants $A$ and $B$ depend on the lepton chirality and the model under consideration. For the minimal Standard Model and the two-doublet model, one can easily see that

$$\begin{array}{lcl} A_L = \frac{3}{4}g^2 + \frac{1}{4}g'^2 & ; & B_L = g_\tau^2 \\ A_R = g'^2 & ; & B_R = 2g_\tau^2 \end{array}, \qquad (13)$$

where the Yukawa contributions are identical for both models, since in either case, the lepton couples to only one scalar doublet. This yields the following thermal lepton masses:

$$\begin{aligned} \Omega_L^2 &= \frac{1}{8v^2}\left(2M_W^2 + M_Z^2 + M_\tau^2\right)T^2 \approx (0.209\,T)^2 && (14) \\ \Omega_R^2 &= \frac{1}{4v^2}\left(2\tan^2\theta_{\rm W}\,M_W^2 + M_\tau^2\right)T^2 \approx (0.127\,T)^2\,. && (15) \end{aligned}$$

Note that $\Omega_L > \Omega_R$; this is true for all leptons $l$, provided that $M_l < 116$ GeV. Also, this result is gauge invariant. The self-energy (7) leads to the following fermion propagator:

$$S(P) = \left[(1+a)\,\not{p} + b\,\not{u}\right]^{-1} = \left[(1+a)\,\not{p} + b\,\not{u}\right]/Z\,, \qquad (16)$$

where the denominator is

$$Z(\omega,p) = (1+a)^2P^2 + 2(1+a)b\,P\cdot u + b^2 = \left[\omega(1+a) + b\right]^2 - \left[p(1+a)\right]^2\,. \qquad (17)$$

The poles of the propagator occur at the zeros of $Z(\omega,p)$,

$$\omega(1+a) + b = \pm p(1+a)\,, \qquad (18)$$

which includes both positive- and negative-energy solutions (note that $(1+a)$ is even, and $b$ odd, under $\omega \to -\omega$); given a positive-energy solution $\omega(p)$, the corresponding negative-energy solution is $-\omega(p)$. So it suffices to find only the positive-energy solutions. The dispersion relation is given by

$$\begin{aligned} \omega \mp p &= -a(\omega,p)(\omega \mp p) - b(\omega,p) \\ &= \frac{\Omega^2}{p}\left[\pm 1 + \frac{1}{2}\left(1 \mp \frac{\omega}{p}\right)\log\left(\frac{\omega+p}{\omega-p}\right)\right]\,. && (19) \end{aligned}$$

Each chirality has two distinct modes, shown in Figure 1, which we label normal ($\omega_+(p)$) and abnormal ($\omega_-(p)$). The abnormal mode is actually unstable for $p \gtrsim \Omega$ [18]. We plot the dispersion relations in Figure 2 for left and right chiralities of the $\tau$-lepton. The dispersion relations may be approximated for small and large $p$ as

$$\frac{\omega_+(p)}{\Omega} \approx \begin{cases} 1 + \frac{1}{3}\frac{p}{\Omega} + \frac{1}{3}\left(\frac{p}{\Omega}\right)^2 & : p \lesssim \Omega \\ \sqrt{2 + \left(\frac{p}{\Omega}\right)^2} & : p \gtrsim \Omega \end{cases} \tag{20}$$

$$\frac{\omega_-(p)}{\Omega} \approx \begin{cases} 1 - \frac{1}{3}\frac{p}{\Omega} + \frac{1}{3}\left(\frac{p}{\Omega}\right)^2 & : p \lesssim \Omega \\ \frac{p}{\Omega}\left[1 + 2\exp\left(-2\left(\frac{p}{\Omega}\right)^2 - 2\right)\right] & : p \gtrsim \Omega \end{cases} . \tag{21}$$

In the broken phase, the Dirac operator is

$$\begin{pmatrix} \Sigma_L^0 + \Sigma_L^b & M \\ M^\dagger & \Sigma_R^0 + \Sigma_R^b \end{pmatrix} , \tag{22}$$

where the thermal piece includes a contribution due to mass corrections in the broken theory:

$$\Sigma_{L,R}^b = \Sigma_{L,R}^s + \delta\Sigma_{L,R} . \tag{23}$$

We then obtain the dispersion relation from

$$\det\begin{pmatrix} \Sigma_L^0 + \Sigma_L^b & M \\ M^\dagger & \Sigma_R^0 + \Sigma_R^b \end{pmatrix} = 0 . \tag{24}$$

The Lagrangian may be made linear for $p \ll \Omega_{L,R}$,

$$\begin{aligned} \mathcal{L}_{\text{eff}} &= 2iL^\dagger\left(\partial_0 - \frac{1}{3}\vec{\sigma}\cdot\vec{\partial} + i\Omega_L\right)L + 2iR^\dagger\left(\partial_0 + \frac{1}{3}\vec{\sigma}\cdot\vec{\partial} + i\Omega_R\right)R \\ &\quad + L^\dagger M R + R^\dagger M^\dagger L , \end{aligned} \tag{25}$$

yielding the dispersion relation

$$\omega(p) = \frac{\Omega_L + \Omega_R}{2} \pm \sqrt{\frac{M^2}{4} + \left(\frac{\Omega_L - \Omega_R}{2} \pm \frac{|\vec{p}|}{3}\right)^2} , \tag{26}$$

where the first $\pm$ is for $L, R$ and the second for normal or abnormal, respectively; the solutions $\omega(p)$ are shown in Figures 3 and 4. Notice that the left abnormal and right normal lines do not intersect (as they do in the symmetric phase), but instead are separated by an energy interval $\Delta\omega = M_\tau$ about the point $\omega_0 = (\Omega_L + \Omega_R)/2$. This interval is the region of total reflection, as we will see below when we consider the scattering of fermions off the bubble wall.

In order to calculate the reflection coefficients, we start from the full Dirac equation,

$$\begin{pmatrix} \Sigma_L^0 + \Sigma_L^s + \delta\Sigma_L & \mathcal{M} \\ \mathcal{M}^\dagger & \Sigma_R^0 + \Sigma_R^s + \delta\Sigma_R \end{pmatrix}\begin{pmatrix} L \\ R \end{pmatrix} = 0 , \tag{27}$$

where $\mathcal{M}(x)$ is the position-dependent mass and embodies the details of the bubble wall profile; in the broken phase $\Sigma^b = \Sigma^s + \delta\Sigma$ and $\mathcal{M} = M$, while in the symmetric phase $\delta\Sigma = 0 = \mathcal{M}$. It is because the left and right chiralities interact differently with the bubble wall that there exists the possibility of seperating C- and CP-odd reflecting currents (weak hypercharge for instance).

As a first approximation, we set $\Sigma^b \approx \Sigma^s$ or $\delta\Sigma \approx 0$, which is plausible since for leptons $M/T \ll 1$; $\delta\Sigma$ includes mass corrections in the one-loop graphs via the propagator $[\not p + M]^{-1}$, where the momentum integrals are dominated by the region $p \sim T$. Again we may linearise the Dirac equation at low momenta, $p \ll \Omega$:

$$\begin{pmatrix} \omega\left(1+\tilde\alpha_L+\tilde\beta_L\right)+i\vec\sigma\cdot\vec\partial(1+\tilde\alpha_L) & \mathcal{M} \\ \mathcal{M}^\dagger & \omega\left(1+\tilde\alpha_R+\tilde\beta_R\right)-i\vec\sigma\cdot\vec\partial(1+\tilde\alpha_R) \end{pmatrix}\begin{pmatrix} L \\ R \end{pmatrix} = 0\,. \tag{28}$$

This may be written as

$$\begin{pmatrix} \sigma^j & 0 \\ 0 & -\sigma^j \end{pmatrix}\frac{\partial\Psi}{\partial x^j} = iUR\Psi\,, \tag{29}$$

where

$$U = \begin{pmatrix} \omega\left(1+\tilde\alpha_L+\tilde\beta_L\right) & \mathcal{M} \\ \mathcal{M}^\dagger & \omega\left(1+\tilde\alpha_R+\tilde\beta_R\right) \end{pmatrix} \tag{30}$$

$$R = \begin{pmatrix} (1+\tilde\alpha_L)^{-1} & 0 \\ 0 & (1+\tilde\alpha_R)^{-1} \end{pmatrix} \tag{31}$$

$$\Psi = R^{-1}\begin{pmatrix} L \\ R \end{pmatrix} \tag{32}$$

$$\tilde\alpha_L = -\frac{1}{3}\frac{\Omega_L^2}{\omega^2}\left(1-3u-2u^2\right)(1-u) \quad ; \quad \tilde\beta_L = -\frac{2}{3}\frac{\Omega_L^2}{\omega^2}(1+u)^2(1-u) \tag{33}$$

$$\tilde\alpha_R = -\frac{1}{3}\frac{\Omega_R^2}{\omega^2}\left(1+3u-2u^2\right)(1+u) \quad ; \quad \tilde\beta_R = -\frac{2}{3}\frac{\Omega_R^2}{\omega^2}(1-u)^2(1+u)\,. \tag{34}$$

A Lorentz transformation from the fluid frame to the wall frame (with velocity $u$) has been performed in the small $u$ limit; the $u$-dependence of $\tilde\alpha$ and $\tilde\beta$ reflect the spinor transformation. Because we are working in the wall frame, the energy and momentum parallel to the wall are conserved: $i\frac{d}{dt} = \omega$, $i\frac{\partial}{\partial x_{\|}} = p_{\|}$. The reflection coefficient depends strongly only on $p_\perp$ (taken to be $p_z$), and so we set $p_{\|} = 0$:

$$\begin{pmatrix} \sigma^3 & 0 \\ 0 & -\sigma^3 \end{pmatrix}\frac{\partial\Psi}{\partial z} = iUR\Psi\,, \tag{35}$$

which decomposes into

$$\frac{\partial}{\partial z}\begin{pmatrix} \psi_1 \\ \psi_3 \end{pmatrix} = i\begin{pmatrix} \omega\left(\frac{1+\tilde\alpha_L+\tilde\beta_L}{1+\tilde\alpha_L}\right) & \mathcal{M}\left(\frac{1}{1+\tilde\alpha_R}\right) \\ -\mathcal{M}^\dagger\left(\frac{1}{1+\tilde\alpha_L}\right) & -\omega\left(\frac{1+\tilde\alpha_R+\tilde\beta_R}{1+\tilde\alpha_R}\right) \end{pmatrix}\begin{pmatrix} \psi_1 \\ \psi_3 \end{pmatrix} \tag{36}$$

$$\frac{\partial}{\partial z}\begin{pmatrix} \psi_4 \\ \psi_2 \end{pmatrix} = i\begin{pmatrix} \omega\left(\frac{1+\tilde\alpha_R+\tilde\beta_R}{1+\tilde\alpha_R}\right) & \mathcal{M}^\dagger\left(\frac{1}{1+\tilde\alpha_L}\right) \\ -\mathcal{M}\left(\frac{1}{1+\tilde\alpha_R}\right) & -\omega\left(\frac{1+\tilde\alpha_L+\tilde\beta_L}{1+\tilde\alpha_L}\right) \end{pmatrix}\begin{pmatrix} \psi_4 \\ \psi_2 \end{pmatrix}\,. \tag{37}$$

This describes reflection and transmission perpendicular to the wall. In analogy to the method of NKC, we write the solution as a path-ordered integral,

$$\begin{pmatrix} \psi_1 \\ \psi_3 \end{pmatrix}(z,t) = e^{-i\omega t}\,\Omega(z)\begin{pmatrix} \psi_1 \\ \psi_3 \end{pmatrix}_0 \tag{38}$$

$$\begin{pmatrix} \psi_4 \\ \psi_2 \end{pmatrix}(z,t) = e^{-i\omega t}\,\overline{\Omega}(z)\begin{pmatrix} \psi_4 \\ \psi_2 \end{pmatrix}_0 , \tag{39}$$

where

$$\Omega(z) = \mathcal{P}\exp i\int_{-z_0}^{z} dx \begin{pmatrix} \omega\left(\frac{1+\tilde{\alpha}_L+\tilde{\beta}_L}{1+\tilde{\alpha}_L}\right) & \mathcal{M}\left(\frac{1}{1+\tilde{\alpha}_R}\right) \\ -\mathcal{M}^\dagger\left(\frac{1}{1+\tilde{\alpha}_L}\right) & -\omega\left(\frac{1+\tilde{\alpha}_R+\tilde{\beta}_R}{1+\tilde{\alpha}_R}\right) \end{pmatrix} \tag{40}$$

$$\overline{\Omega}(z) = \mathcal{P}\exp i\int_{-z_0}^{z} dx \begin{pmatrix} \omega\left(\frac{1+\tilde{\alpha}_R+\tilde{\beta}_R}{1+\tilde{\alpha}_R}\right) & \mathcal{M}^\dagger\left(\frac{1}{1+\tilde{\alpha}_L}\right) \\ -\mathcal{M}\left(\frac{1}{1+\tilde{\alpha}_R}\right) & -\omega\left(\frac{1+\tilde{\alpha}_L+\tilde{\beta}_L}{1+\tilde{\alpha}_L}\right) \end{pmatrix} . \tag{41}$$

We denote the path-ordered exponentials by

$$\Omega(z) = \mathcal{P}\exp i\int_{-z_0}^{z} dx\; Q(x) \tag{42}$$

$$\overline{\Omega}(z) = \mathcal{P}\exp i\int_{-z_0}^{z} dx\; \overline{Q}(x) . \tag{43}$$

Note that $\Omega$ and $\overline{\Omega}$ satisfy the differential equations $\frac{d\Omega}{dz} = iQ$ and $\frac{d\overline{\Omega}}{dz} = i\overline{Q}$. $\Omega$ describes $L \to R$ reflection and $R \to R$ transmission, while $\overline{\Omega}$ describes $R \to L$ reflection and $L \to L$ transmission. As a first approximation, we take the wall profile to be described by a step-function:

$$\mathcal{M} = \begin{cases} M & : z > 0 \\ 0 & : z < 0 \end{cases} . \tag{44}$$

Then in the symmetric phase,

$$\Omega(z<0) = \begin{pmatrix} \exp i\omega\left(\frac{1+\tilde{\alpha}_L+\tilde{\beta}_L}{1+\tilde{\alpha}_L}\right) z & 0 \\ 0 & \exp -i\omega\left(\frac{1+\tilde{\alpha}_R+\tilde{\beta}_R}{1+\tilde{\alpha}_R}\right) z \end{pmatrix} \equiv \begin{pmatrix} \exp ip_L^{\mathrm{s}} z & 0 \\ 0 & \exp -ip_R^{\mathrm{s}} z \end{pmatrix} , \tag{45}$$

while in the broken phase, $\Omega$ may be diagonalised as

$$\Omega(z>0) = D^{-1}\begin{pmatrix} \exp ip_L^{\mathrm{b}} z & 0 \\ 0 & \exp -ip_R^{\mathrm{b}} z \end{pmatrix} D , \tag{46}$$

where the momenta in the broken phase are

$$\pm\, p_{L,R}^{\mathrm{b}} = \frac{p_L^{\mathrm{s}} - p_R^{\mathrm{s}}}{2} \pm \sqrt{\left(\frac{p_L^{\mathrm{s}} + p_R^{\mathrm{s}}}{2}\right)^2 - \frac{M^2}{(1+\tilde{\alpha}_L)(1+\tilde{\alpha}_R)}} . \tag{47}$$

Then

$$D\begin{pmatrix}\psi_1\\ \psi_3\end{pmatrix}(z>0)=\begin{pmatrix}\exp ip_L^{\rm b}z & 0\\ 0 & \exp -ip_R^{\rm b}z\end{pmatrix}D\begin{pmatrix}\psi_1\\ \psi_3\end{pmatrix}(0)\,, \tag{48}$$

with the diagonalisation matrix given by

$$D=\begin{pmatrix}\frac{1}{Y}(\varpi+\sqrt{B}) & \frac{1}{Y}\left(\frac{M}{1+\tilde{\alpha}_R}\right)\\ \frac{1}{X}\left(\frac{M}{1+\tilde{\alpha}_L}\right) & \frac{1}{X}\left(\varpi+\sqrt{B}\right)\end{pmatrix}, \tag{49}$$

where

$$\varpi = \frac{p_L^{\rm s}+p_R^{\rm s}}{2} \tag{50}$$

$$B = \varpi^2-\frac{M^2}{(1+\tilde{\alpha}_L)(1+\tilde{\alpha}_R)}\,. \tag{51}$$

Here $X$ and $Y$ are just normalisation constants. The reflection coefficient comes from the condition

$$\begin{pmatrix}T\\ 0\end{pmatrix}=D\begin{pmatrix}1\\ R\end{pmatrix}, \tag{52}$$

yielding

$$\mathcal{R}_{L\to R}=|R|^2_{L\to R}=\left|\frac{1+\tilde{\alpha}_R}{1+\tilde{\alpha}_L}\right|\left|\frac{\varpi-\sqrt{B}}{\varpi+\sqrt{B}}\right|\,. \tag{53}$$

Similarly, the right-to-left reflection coefficient may be found from the Dirac equation (37) for $\psi_2$ and $\psi_4$, with the result

$$\mathcal{R}_{R\to L}=\left|\frac{1+\tilde{\alpha}_L}{1+\tilde{\alpha}_R}\right|\left|\frac{\varpi-\sqrt{B}}{\varpi+\sqrt{B}}\right|\,. \tag{54}$$

Note that $\mathcal{R}_{L\to R}\approx\mathcal{R}_{R\to L}\approx 1$ if $\sqrt{B}$ is imaginary; that is, if

$$\varpi^2<\frac{M^2}{(1+\tilde{\alpha}_L)(1+\tilde{\alpha}_R)}, \tag{55}$$

we get *total reflection.* In physical terms, an imaginary contribution to the momentum (47) implies an evanescent (decaying exponential) transmission amplitude in the broken phase.

Although the step-function wall profile may produce spurious effects due to its discontinuity, Farrar and Shaposhnikov considered the smooth profile

$$\mathcal{M}^2=\frac{M^2}{1+e^{-az}}, \tag{56}$$

and found the reflection coefficients

$$\begin{aligned}\mathcal{R}_{L\to R} &= \left|\frac{1+\tilde{\alpha}_R}{1+\tilde{\alpha}_L}\right|\left|\frac{\sinh\frac{\pi}{a}(\varpi-\sqrt{B})}{\sinh\frac{\pi}{a}(\varpi+\sqrt{B})}\right|\\ \mathcal{R}_{R\to L} &= \left|\frac{1+\tilde{\alpha}_L}{1+\tilde{\alpha}_R}\right|\left|\frac{\sinh\frac{\pi}{a}(\varpi-\sqrt{B})}{\sinh\frac{\pi}{a}(\varpi+\sqrt{B})}\right|\,.\end{aligned} \tag{57}$$

Notice that total reflection again appears for $\bar{\omega}^2 < M^2/(1+\tilde{\alpha}_L)(1+\tilde{\alpha}_R)$. We will take this as a general condition for total reflection (like the condition $\omega < M$ for the zero-temperature case). The region of total reflection is shown in Figure 5. As expected by comparison to the dispersion relations in the broken phase (Figure 4), total reflection occurs in the energy interval of width $\Delta\omega \sim M$ about $\omega_0 \sim (\Omega_L + \Omega_R)/2$; the deviation results from the dependence of the reflection coefficients on the wall velocity $u$.

Using this result we are now able to compute the hypercharge flux reflected off the bubble wall. We neglect quarks, since we assume that the primordial baryon asymmetry vanishes and that CP violation in the CKM matrix is inadequate to produce the observed baryon number. We need to calculate

$$\begin{aligned} f_Y &= -\frac{1}{2}f_{\tau_L} + \frac{1}{2}f_{\bar{\tau}_R} - f_{\tau_R} + f_{\bar{\tau}_L} - \frac{1}{2}f_{\nu_\tau} + \frac{1}{2}f_{\bar{\nu}_\tau} \\ &\quad + (\mu\text{-contribution}) + (e\text{-contribution})\ . \end{aligned} \tag{58}$$

Because $M_\tau \gg M_\mu, M_e$, the interactions of the muon and electron families with the bubble wall are negligible compared to those of the tau family, and hence their contributions to the reflected flux may be ignored. In the following, $f_{\tau_L}$ denotes the $\tau_L$ particle flux in the fluid frame, while $f_L^{s,b}$ denotes the $\tau_L$ number density distributions in the wall frame, for the symmetric and broken phases; and similarly for the other species. To find $f_j$, the particle flux in the thermal (fluid) frame, we compute the flux $\gamma f_j$ in the wall frame ($\gamma = 1/\sqrt{1-u^2}$, where $u$ is the wall velocity):

$$\gamma f_{\tau_L} = \int \frac{d^3k}{(2\pi)^3}\, [f_R^s(k_L, k_T)\cdot \mathcal{R}_{R\to L}(\omega)] \tag{59}$$

$$\gamma f_{\bar{\tau}_R} = \int \frac{d^3k}{(2\pi)^3}\, [f_{\bar{L}}^s(k_L, k_T)\cdot \mathcal{R}_{\bar{L}\to \bar{R}}(\omega)]\ . \tag{60}$$

The integrals are taken over particle momenta in the wall frame and by CPT and Lorentz invariance, $\mathcal{R}_{\bar{L}\to\bar{R}} = \mathcal{R}_{L\to R}$. There is no term for reflection off the symmetric phase because the dispersion curves for left-abnormal and right-normal modes intersect in the symmetric phase; see Figure 2. Also there is no term for particle transmission from the broken phase since it is assumed that both the broken and symmetric phases have zero net hypercharge, so that the transmitted hypercharge flux is zero when summed over all particle species. Thus reflection yields the only substantial hypercharge flux, and in particular, the contribution from total reflection dominates. The difference of these integrals may be written as

$$f_{\tau_L} - f_{\bar{\tau}_R} = \frac{1}{\gamma}\int \frac{d^3k}{(2\pi)^3}\, [f_R^s\,(\mathcal{R}_{R\to L} - \mathcal{R}_{L\to R}) + (f_R^s - f_{\bar{L}}^s)\,\mathcal{R}_{L\to R}]\ . \tag{61}$$

The first term is much smaller (by a factor of $\sim 10$) than the second since the difference in reflection coefficients results from the difference in the left and right thermal masses. We shall therefore omit it in the remainder of this discussion for the sake of clarity.

The above integral is dominated by the region of total reflection, $\mathcal{R} \approx 1$, which (as we have seen above) occurs for $B < 0$ or

$$\overline{\omega}^2 < \frac{M^2}{(1+\tilde{\alpha}_L)(1+\tilde{\alpha}_R)} , \tag{62}$$

and the hypercharge flux is therefore governed by the $\tau$-lepton;

$$\begin{aligned} f_Y &\approx -\frac{1}{2}(f_{\tau_L} - f_{\bar{\tau}_R}) - (f_{\tau_R} - f_{\bar{\tau}_L}) \\ &\approx -\frac{1}{\gamma}\int \frac{d^3k}{(2\pi)^3} \left\{ \frac{1}{2}(f^s_R - f^s_{\bar{L}}) \cdot \mathcal{R}_{L\to R} + (f^s_L - f^s_{\bar{R}}) \cdot \mathcal{R}_{R\to L} \right\} \\ &\approx -\frac{1}{\gamma}\int_{B<0} \frac{d^3k}{(2\pi)^3} \left\{ \frac{1}{2}(f^s_R - f^s_{\bar{L}}) + (f^s_L - f^s_{\bar{R}}) \right\} . \end{aligned} \tag{63}$$

The flux distributions are taken in the wall frame;

$$f^s_j = \frac{\partial \omega_j}{\partial k_z} \cdot n_F\left(\gamma\left[\omega_j - uP^z_j\right] \mp \mu_j\right) , \tag{64}$$

where the group momentum and fermion particle distribution (in the thermal frame) are

$$P^z_j = \omega_j \frac{\partial \omega_j}{\partial k_z} \tag{65}$$

$$n_F(\omega \mp \mu) = \frac{1}{e^{(\omega\mp\mu)/T} + 1} . \tag{66}$$

Substituting into eq.(63) gives

$$\begin{aligned} f_Y \approx -\frac{1}{\gamma}\int_{B<0} \frac{d^3k}{(2\pi)^3} &\left\{ \frac{1}{2}\frac{\partial \omega_R}{\partial k_z}\left[n_F\left(\gamma[\omega_R - uP^z_R] - \mu_{\tau_R}\right) - n_F\left(\gamma[\omega_R - uP^z_{\bar{R}}] + \mu_{\tau_R}\right)\right] \right. \\ &\left. + \frac{\partial \omega_L}{\partial k_z}\left[n_F\left(\gamma[\omega_L - uP^z_L] - \mu_{\tau_L}\right) - n_F\left(\gamma[\omega_L - uP^z_{\bar{L}}] + \mu_{\tau_L}\right)\right] \right\} . \end{aligned} \tag{67}$$

As a conservative estimate, we truncate the region of phase space where $B < 0$ to the region where $k_{||} \lesssim \frac{3}{2}(\Omega_L - \Omega_R)$ and $\partial\omega_{L,R}/\partial k_{||} \approx 0$ (see FS for a discussion on this point). The $k_{||}$- and $k_z$-integrals can now be separated, giving the result

$$\begin{aligned} f_Y \approx -\frac{9}{16\pi\gamma}\Delta\omega\,(\Omega_L - \Omega_R)^2 &\left\{ \frac{1}{2}\Delta n_F\left(\gamma\left[\omega_0 - uP^z_{\bar{R}}\right] \mp \mu_{\tau_R}\right) \right. \\ &\left. + \Delta n_F\left(\gamma\left[\omega_0 - uP^z_{\bar{L}}\right] \mp \mu_{\tau_L}\right) \right\} , \end{aligned} \tag{68}$$

where the region of total reflection is centered about $\omega_0$ with spread $\Delta\omega$. To lowest order in the chemical potentials $\mu_{\tau_L,\tau_R}/T$,

$$\begin{aligned}\Delta n_F\left(\gamma\left[\omega_0 - uP^z_j\right] \mp \mu_j\right) &= n_F\left(\gamma\left[\omega_0 - uP^z_j\right] - \mu_j\right) - n_F\left(\gamma\left[\omega_0 - uP^z_j\right] + \mu_j\right) \\ &\approx \frac{\mu_j/T}{1+\cosh\left(\frac{\gamma(\omega_0 - uP^z_j)}{T}\right)} ,\end{aligned} \tag{69}$$

and in the limit of small $u$ and $k_{\|}$,

$$P^z \approx \frac{\omega_0}{3}(1+2u/3) , \tag{70}$$

hence

$$\frac{1}{2}\Delta n_F\left(\gamma\left[\omega_0 - uP^z_R\right] \mp \mu_{\tau_R}\right) + \Delta n_F\left(\gamma\left[\omega_0 - uP^z_L\right] \mp \mu_{\tau_L}\right) \approx \frac{1}{2}\cdot\frac{(\mu_{\tau_R}+2\mu_{\tau_L})/T}{1+\cosh\left(\frac{\omega_0}{T}(1-u/3)\right)} . \tag{71}$$

Noticing that $\rho_\tau = (\mu_{\tau_R}+2\mu_{\tau_L})T^2/6$ (refer to the following section), we find that $f_Y$ is simply proportional to the primordial $\tau$-lepton asymmetry. Our final result for the reflected hypercharge flux is then

$$f_Y \approx -\frac{27}{16\pi}\cdot\frac{(\Omega_L-\Omega_R)^2\Delta\omega}{T^3}\cdot\frac{\rho_\tau}{1+\cosh\left(\frac{\omega_0}{T}(1-u/3)\right)} . \tag{72}$$

We believe this expression to be a conservative lower bound, since we have truncated the flux integral (68) in the region of total reflection and we have neglected the contribution of $k_{\|}\sim\omega_0$.

# Partial Derivative of the Free Energy ($\partial F/\partial B$)

We now compute $\partial F/\partial B$, the partial derivative of the free energy with all conserved quantum numbers held fixed. We cannot simply adopt the result of NKC, since their analysis implies not only $B=L=0$, but also $B_j=L_j=0$ for the individual generations. Since we are interested in the case of generational differences in lepton asymmetries, we redo the analysis.

$\partial F/\partial B$ depends on the interactions and species in equilibrium. We assume that on the timescale $\tau_T$, $SU(3)_C\otimes SU(2)_L\otimes U(1)_Y$ interactions are in equilibrium (including quark mixing and light-fermion Yukawa interactions, which are assumed to be out of equilibrium in the NKC analysis), and that only the anomalous $B+L$-violation is not in equilibrium. The (approximately) conserved quantum numbers and their associated chemical potentials are then

$$\begin{aligned} B/3 - L_j &\leftrightarrow \mu_j \\ B &\leftrightarrow \mu_B \\ Y/2 &\leftrightarrow \mu_Y \\ T_3 &\leftrightarrow \mu_T .\end{aligned}$$

This implies that on the timescale of interest, $Q$, $L_j$, and $B \pm L$ are also conserved. In contrast NKC had $B_1 = B_2$ and $B_3$ separately conserved, and $L_j = L/3$; when the constraints $B = 0 = L$ and $B_1 = B_2 = 0$ were imposed, one obtained $B_j = 0 = L_j$. In our case we have $L_j$ conserved and $B_j = B/3$, and the constraints we impose are $B = 0 = L$, so that $B_j = 0$ although $L_j \neq 0$ is allowed. The net particle number densities are

$$
\begin{aligned}
\rho_{t_L} &= 3\left[\frac{1}{9}(\mu_1+\mu_2+\mu_3)+\frac{1}{3}\mu_B+\frac{1}{6}\mu_Y+\frac{1}{2}\mu_T\right]\frac{T^2}{6} \\
\rho_{b_L} &= 3\left[\frac{1}{9}(\mu_1+\mu_2+\mu_3)+\frac{1}{3}\mu_B+\frac{1}{6}\mu_Y-\frac{1}{2}\mu_T\right]\frac{T^2}{6} \\
\rho_{t_R} &= 3\left[\frac{1}{9}(\mu_1+\mu_2+\mu_3)+\frac{1}{3}\mu_B+\frac{2}{3}\mu_Y\right]\frac{T^2}{6} \\
\rho_{b_R} &= 3\left[\frac{1}{9}(\mu_1+\mu_2+\mu_3)+\frac{1}{3}\mu_B-\frac{1}{3}\mu_Y\right]\frac{T^2}{6} \\
\rho_{c_L} &= \rho_{u_L} = \rho_{t_L} \quad ; \quad \rho_{s_L} = \rho_{d_L} = \rho_{b_L} \\
\rho_{c_R} &= \rho_{u_R} = \rho_{t_R} \quad ; \quad \rho_{s_R} = \rho_{d_R} = \rho_{b_R} \\
\rho_{e_L} &= \left(-\mu_1-\frac{1}{2}\mu_Y-\frac{1}{2}\mu_T\right)\frac{T^2}{6} \quad ; \quad \rho_{\nu_e} = \left(-\mu_1-\frac{1}{2}\mu_Y+\frac{1}{2}\mu_T\right)\frac{T^2}{6} \\
\rho_{\mu_L} &= \left(-\mu_2-\frac{1}{2}\mu_Y-\frac{1}{2}\mu_T\right)\frac{T^2}{6} \quad ; \quad \rho_{\nu_\mu} = \left(-\mu_2-\frac{1}{2}\mu_Y+\frac{1}{2}\mu_T\right)\frac{T^2}{6} \\
\rho_{\tau_L} &= \left(-\mu_3-\frac{1}{2}\mu_Y-\frac{1}{2}\mu_T\right)\frac{T^2}{6} \quad ; \quad \rho_{\nu_\tau} = \left(-\mu_3-\frac{1}{2}\mu_Y+\frac{1}{2}\mu_T\right)\frac{T^2}{6} \\
\rho_{e_R} &= (-\mu_1-\mu_Y)\frac{T^2}{6} \quad ; \quad \rho_{\mu_R} = (-\mu_2-\mu_Y)\frac{T^2}{6} \quad ; \quad \rho_{\tau_R} = (-\mu_3-\mu_Y)\frac{T^2}{6} \\
\rho_{\phi^+} &= n(\mu_Y+\mu_T)\frac{T^2}{6} \quad ; \quad \rho_{\phi^0} = n(\mu_Y-\mu_T)\frac{T^2}{6} \\
\rho_{W^+} &= 4\mu_T\frac{T^2}{6}\,.
\end{aligned}
$$

In the above, $n$ denotes the number of scalar doublets in equilibrium. Then

$$
\begin{aligned}
\frac{\rho_Y}{2} &= 3\cdot\frac{1}{6}(\rho_{t_L}+\rho_{b_L})+3\cdot\frac{2}{3}\rho_{t_R}-3\cdot\frac{1}{3}\rho_{b_R} \\
&\quad -\frac{1}{2}\left(\rho_{e_L}+\rho_{\mu_L}+\rho_{\tau_L}+\rho_{\nu_e}+\rho_{\nu_\mu}+\rho_{\nu_\tau}\right) \\
&\quad -(\rho_{e_R}+\rho_{\mu_R}+\rho_{\tau_R})+\frac{1}{2}(\rho_{\phi^+}+\rho_{\phi^0}) \\
&= \left[\frac{8}{3}(\mu_1+\mu_2+\mu_3)+2\mu_B+(10+n)\mu_Y\right]\frac{T^2}{6} \\
\rho_{T_3} &= (10+n)\mu_T\frac{T^2}{6} \\
\rho_B &= 3\cdot\frac{1}{3}(\rho_{t_L}+\rho_{b_L}+\rho_{t_R}+\rho_{b_R}) \\
&= \left[\frac{4}{3}(\mu_1+\mu_2+\mu_3)+4\mu_B+2\mu_Y\right]\frac{T^2}{6}
\end{aligned}
$$

$$
\begin{aligned}
\rho_L &= \rho_{e_L} + \rho_{\mu_L} + \rho_{\tau_L} + \rho_{\nu_e} + \rho_{\nu_\mu} + \rho_{\nu_\tau} + \rho_{e_R} + \rho_{\mu_R} + \rho_{\tau_R} \\
&= [-3(\mu_1 + \mu_2 + \mu_3) - 6\mu_Y]\,\frac{T^2}{6} \\
\rho_{L_j} &= (-3\mu_j - 2\mu_Y)\,\frac{T^2}{6} = [-3\mu_j + (\mu_1 + \mu_2 + \mu_3)]\,\frac{T^2}{6}\,. \qquad (73)
\end{aligned}
$$

Imposing the conditions $B = 0 = L$, we find

$$
\begin{aligned}
\mu_Y &= 6\mu_B \\
\mu_1 + \mu_2 + \mu_3 &= -12\mu_B\,,
\end{aligned}
$$

giving

$$
\frac{\partial F}{\partial B} = \mu_B = \frac{\rho_Y}{(5+n)T^2} \equiv \frac{\xi \rho_Y}{T^2}\,. \qquad (74)
$$

# Thermal Transport Time ($\tau_T$)

After rebounding off the bubble wall, the reflected lepton flux travels into the symmetric phase until the advancing front of broken phase captures it, during which time the corresponding hypercharge current biases baryon production via anomalous processes. We now estimate the thermal transport time $\tau_T$, defined as the average time that a reflected $\tau$-lepton spends in the plasma prior to absorption by the bubble of broken phase. Consider diffusion away from the wall of a particle with velocity $v$ and mean free path $l$. Capture occurs when the wall intercepts the randomly walking particle ($N$ here is the number of collisions):

$$
u\tau_T = \left\langle l\sqrt{N} \right\rangle = \left\langle l\sqrt{\frac{v\tau_T}{l}} \right\rangle\,, \qquad (75)
$$

or

$$
\tau_T = \left\langle \frac{lv}{u^2} \right\rangle\,. \qquad (76)
$$

We therefore need to calculate the thermal average

$$
\langle lv \rangle = \left\langle \frac{v}{\langle n\sigma \rangle_1} \right\rangle_2\,, \qquad (77)
$$

where the subscripts 1 and 2 refer to thermal averages taken over the rebounding particles and particles in the plasma, respectively. Here $n$ is the particle number density and $\sigma$ the thermally averaged cross section. The thermal transport time may then be written as

$$
\tau_T^{-1} = \sum_2 \frac{u^2 g_1 g_2}{\langle n \rangle_1} \int \frac{d^3\vec{p}_1\, d^3\vec{p}_2}{(2\pi)^6}\, \frac{E_1}{|\vec{p}_1|}\, \frac{\sigma_{12}(\vec{p}_1, \vec{p}_2)}{(e^{E_1/T}+1)(e^{E_2/T}+1)}\,, \qquad (78)
$$

where the sum is taken over all interactions of particle 1 with the heat bath and $g_j$ counts the spin degrees of freedom. Since the leptons only interact electroweakly, it is reasonable to approximate the above expression by considering only the leading contributions from tree-level scattering on mass shell. Numerical calculation confirms that other contributions are indeed less significant. In this case, the transition probabilities sum to

$$\sum |T|^2 \approx \frac{e^2}{\sin^2\theta_W}\left(\Omega_W^2 - \Omega_\tau^2\right) \tag{79}$$

$$+ \frac{e^2}{\sin^2\theta_W \cos^2\theta_W}\left(4\sin^4\theta_W\,\Omega_W^2 + 8\sin^4\theta_W\,\Omega_\tau^2 - 2\sin^2\theta_W\,\Omega_W^2\right. \tag{80}$$

$$\left. - 4\sin^2\theta_W\,\Omega_\tau^2 + \Omega_W^2 - \Omega_\tau^2\right) \tag{81}$$

$$+ 4e^2\left(\Omega_\gamma^2 + \Omega_\tau^2\right) , \tag{82}$$

where we respectively list the contributions of $W$, $Z$, and $\gamma$ scattering in the plasma (higgs scattering is negligible since it is suppressed by the small Yukawa couplings). $\Omega_j$ is the thermal mass of particle species $j$, and we have set $\Omega_\gamma \approx \Omega_W \approx 0.5T$ and $\Omega_{\nu_\tau} \approx \Omega_\tau \approx 0.2T$. The thermal transport time is then given by

$$\tau_T \equiv \frac{x}{u^2T} \sim \frac{100}{u^2T} . \tag{83}$$

Note that, computing $\langle v\rangle = \langle nv\rangle/\langle n\rangle$, we find that $v \approx 1$ for most leptons in the plasma, which confirms that the reflected lepton current is quickly thermalised.

# Discussion

Taking the expression (5) for the final baryon number and substituting in eqs.(72), (74), and (83) for the reflected hypercharge flux, the partial derivative of the free energy with respect to baryon number, and the thermal transport time, we obtain

$$\begin{aligned}
\frac{\rho_B}{s} &\approx \frac{81}{16\pi}\cdot\frac{\kappa\alpha_W^4}{(5+n)u^3}\cdot\frac{x\left(\Omega_L-\Omega_R\right)^2\Delta\omega}{T^3\left[1+\cosh\frac{\omega_0}{T}(1-u/3)\right]}\cdot\left(\frac{\rho_\tau}{s}\right)\\
&\approx 2.1\cdot 10^{-6}\cdot\frac{\kappa x}{(5+n)u^3\left[1+\cosh\frac{\omega_0}{T}(1-u/3)\right]}\cdot\frac{\left(\Omega_L-\Omega_R\right)^2 M_\tau}{T^3}\cdot\left(\frac{\rho_\tau}{s}\right)\\
&\approx 2.1\cdot 10^{-6}\cdot\kappa\left(\frac{6}{5+n}\right)\left(\frac{0.1}{u}\right)^3\left(\frac{100\,\mathrm{GeV}}{T}\right)\left(\frac{2}{1+\cosh\frac{\omega_0}{T}(1-u/3)}\right)\left(\frac{x}{100}\right)\cdot\left(\frac{\rho_\tau}{s}\right) ,
\end{aligned} \tag{84}$$

where the various parameters have been scaled by their typical values. We believe eq.(84) to be a conservative lower bound on the effect of this mechanism since we have underestimated the flux integrals. By requiring the observed baryon number of $\rho_B \sim 10^{-10}$ to be generated in this manner, we obtain an estimate for the primordial lepton asymmetry,

$$\frac{\rho_\tau}{s} \sim 5\cdot 10^{-5} , \tag{85}$$

for the typical values of parameters ($\kappa = 1$, $u = 0.1$, $x = 100$). This corresponds to

$$\frac{n_l - n_{\bar{l}}}{n_l + n_{\bar{l}}} \sim 0.005 . \tag{86}$$

It is of interest to compare this constraint with that obtained from equilibrium scenarios for lepton-to-baryon conversion. As a generic example, we consider the analysis of Kuzmin, Rubakov, and Shaposhnikov [8]. Taking the requisite large Higgs mass to be $M_H \sim 100$ GeV, and consequently the sphaleron freeze-out temperature (approximately the critical temperature) to be $T_* \sim 150$ GeV, we estimate the generated baryon asymmetry as

$$\frac{\rho_B}{s} \approx -\frac{4}{13\pi^2}\frac{m_\tau^2}{T_*^2} \cdot \left(\frac{\rho_\tau}{s}\right) \approx -4.4 \cdot 10^{-6} \cdot \left(\frac{\rho_\tau}{s}\right) . \tag{87}$$

Hence the observed baryon asymmetry may be accounted for in this scheme for a primordial lepton asymmetry of $\rho_\tau/s \sim 2 \cdot 10^{-5}$, which is remarkably similar to the value found above despite the $m_\tau^2/T^2$ suppression. This is not surprising since, as we have emphasised, the assumption that baryon violation is in equilibrium (on the timescale of interest) is an overly optimistic one.

A remark is in order about the behaviour of eq.(84) as $u \to 0$. In contrast to NKC, our result diverges unashamedly at low wall velocity as $\sim 1/u^3$. To see why this is acceptable, consider the extreme case of a stationary wall. In this case the $\tau$-leptons simply diffuse away from the wall, finally establishing equilibrium once the hypercharge profile is constant (and different) on either side. In this sense the wall is behaving like a semi-permeable membrane since it forces different partial pressures of leptons on the outside and inside of the bubble. Intuitively, one expects the partial pressure of leptons in the symmetric phase to create baryons via sphaleron transitions until it is fully depleted. However in this calculation we have made an approximation by setting the chemical potentials to be constant. This means an unlimited supply of lepton number – hence the divergence. Our approximation breaks down once the wall velocity is slow enough so that the lepton numbers are depleted significantly. This condition can be gauged by the ratio of generated density of baryons to initial density of leptons. This is a small number for $u \gtrsim 0.001$ which gives a sufficient range of values for first order phase transitions (where $u \gtrsim 0.01$ is more reasonable)[17]. Clearly, in this scenario, the slower the wall velocity the more efficient the mechanism.

To summarise, we have considered the generation of baryons from a primordial $\tau$-lepton asymmetry. There are two ways in which baryogenesis may occur which give remarkably similar results. The first is already well known in the literature, and assumes that the thermal plasma maintains equilibrium during the electro-weak phase transition. Anomalous processes may convert generational lepton asymmetries into baryon number, whose final value depends on the primordial asymmetry. The effectiveness of this scenario is determined by the suppression factor $M_l^2(T_*)/T_*^2$ at sphaleron freeze-out. We have analysed a second mechanism, which would operate during a first-order phase transition. Reflection of $\tau$-leptons off the phase separation boundary may radiate a net hypercharge flux, which then triggers baryon production as described by the rate equation (1). The effectiveness of this charge transport mechanism is determined by the strength of the lepton Yukawa interactions with the bubble wall, through the factor $M_l/T$. This mechanism works most efficiently for slow wall velocities. Although a comparison between the two depends on the choice of parameter values, there is a clear trade-off between opposing tendencies: anomalous baryon violation in equilibrium generates greater net $B$, but risks suppression by lepton mass effects. We have made several assumptions in deriving the final baryon number, which we summarise:

- the reflected hypercharge flux is dominated by the contribution due to total reflection;
- the linearised (low-momentum) Lagrangian is valid in the region of total reflection;
- the wall velocity is non-relativistic (implying that the hypercharge current rapidly thermalises);
- the flux integrals may be approximated by $k_{\|} \lesssim \frac{3}{2}(\Omega_L - \Omega_R)$.

The last assumption together with the parameters $\kappa$, $u$ and $x$ are the greatest unknowns. For typical values, we have found that the observed baryon number of $\rho_B \sim 10^{-10}$ may be generated by our mechanism, if the primordial lepton asymmetry is $\rho_\tau/s \sim \mathcal{O}(10^{-5})$.

Finally, we note that scalar leptons in supersymmetry, may play a similar role to the $\tau$-lepton above. After finding the quasiparticle modes and dispersion relations by diagonalising the mass matrices in both the symmetric and broken phases, one may analyse the scattering of sleptons off the bubble wall in the fashion described above. We expect that a region of total reflection of width $\Delta\omega \sim M_\tau$ would again yield an $M_\tau/T$-suppressed contribution to the reflected hypercharge flux, in the manner demonstrated. This is in contrast to the equilibrium case examined in ref.[9], where the minimal supersymmetric extension of the Standard Model produces a much greater enhancement due to the large mass splittings of right and left sleptons.

**Acknowledgement** We would like to thank Herbi Dreiner and Noel Cottingham for stimulating discussions.

# References


[1] G. 't Hooft, *Phys. Rev. Lett.* **37** (1976) 8

[2] N. S. Manton, *Phys. Rev.* **D28** (1983) 2019; F. R. Klinkhamer and N. S. Manton, *Phys. Rev.* **D30** (1984) 2212

[3] N. Turok and J. Zadrozny, *Phys. Rev. Lett.* **65** (1990) 2331; *Nucl. Phys.* **B358** (1991) 471; L. McLerran, M. E. Shaposhnikov, N. Turok, and M. Voloshin, *Phys. Lett.* **256B** (1991) 451; A. G. Cohen and D. B. Kaplan,*Phys. Lett.* **B199** (1987) 251; *Nucl. Phys.* **B308** (1988) 913; A. G. Cohen, D. B. Kaplan and A. E. Nelson, *Phys. Lett.* **B263** (1991) 86; S. A. Abel, W. N. Cottingham and I. B. Whittingham, *Nucl. Phys.* **B410** (1993) 173; A. G. Cohen and A. E. Nelson, *Phys. Lett.* **297B**(1992) 111; A. G. Cohen, D. B. Kaplan and A. E. Nelson, *Nucl. Phys.* **B349** (1991) 727; M. E. Shaposhnikov, Report No. CERN-TH.6497/92; A. G. Cohen, D. B. Kaplan, and A. E. Nelson, Report No. BUHEP-93-4

[4] A. E. Nelson, D. B. Kaplan and A. G. Cohen, *Nucl. Phys.* **B373** (1992) 453

[5] M. Dine, R. G. Leigh, P. Huet, A. Linde and D. Linde, *Phys. Rev.* **D46** (1992) 550; K. E. C. Benson, *Phys. Rev.* **D48** (1993) 2456

[6] K. Kajantie, K. Rammukainen and M. E. Shaposhnikov, Report No. CERN-TH.6901/93; M. E. Shaposhnikov, Report No. CERN-TH.6981/93

[7] M. Fukugita and T. Yanagida, *Phys. Lett.* **B174** (1986) 45; J. A. Harvey and M. S. Turner, *Phys. Rev.* **D42** (1990) 3344

[8] V. A. Kuzmin, V. A. Rubakov, and M. E. Shaposhnikov, *Phys. Lett.* **B191** (1987) 171

[9] H. Dreiner and G. G. Ross, *Nucl. Phys.* **B410** (1993) 188

[10] M. Luty, *Phys. Rev.* **D45** (1991) 455

[11] B. A. Campbell, S. Davidson, J. Ellis, and K. A. Olive, *Phys. Lett.* **B297** (1992) 118

[12] G. R. Farrar and M. E. Shaposhnikov, Report No. CERN-TH.6732/93.

[13] M. Pietroni, *Nucl. Phys.* **B402** (1993) 27

[14] M. Dine, O. Lechtenfeld, B. Sakita, W. Fischler, and J. Polchinski, *Nucl. Phys.* **B342** (1990) 381

[15] P. Arnold and L. McLerran, *Phys. Rev.* **D36** (1987) 581; *Phys. Rev.* **D37** (1988) 1020; S. Y. Khlebnikov and M. E. Shaposhnikov, *Nucl. Phys.* **B308** (1988) 885; L. Carson, X. Li, L. McLerran, and R. T. Wang, *Phys. Rev.* **D42** (1990) 2127

[16] J. Ambjorn, T. Askaard, H. Porter, and M. E. Shaposhnikov, *Phys. Lett.* **B244** (1990) 479; *Nucl. Phys.* **B353** (1991) 346; J. Ambjorn and K. Farakos, *Phys. Lett.* **294B** (1992) 248

[17] B. H. Liu, L. McLerran and N. Turok, *Phys. Rev.* **D46** (1992) 2668

[18] H. A. Weldon, *Phys. Rev.* **D26** (1982) 1394; *Phys. Rev.* **D26** (1982) 2789; V. V. Lebedev and A. V. Smilga, *Ann. Phys.* **202** (1990) 229

# FIGURE CAPTIONS

Figure 1 : The dispersion relations for normal and abnormal plasma modes in the symmetric phase.

Figure 2 : The dispersion relations for left and right chiralities of the $\tau$-lepton in the symmetric phase of the Standard Model and two-doublet model.

Figure 3 : The dispersion relations, at low momenta in the broken phase, for normal and abnormal modes of left and right chiralities of the $\tau$-lepton in the Standard Model and two-doublet model.

Figure 4 : Close-up of the previous figure, magnifying the separation between the left abnormal and right normal lines.

Figure 5 : The region of total reflection (bounded by the curves plotted) for the $\tau$-lepton in the Standard Model and two-doublet model, as a function of the wall velocity; the temperature is taken to be $T = 100$ GeV.

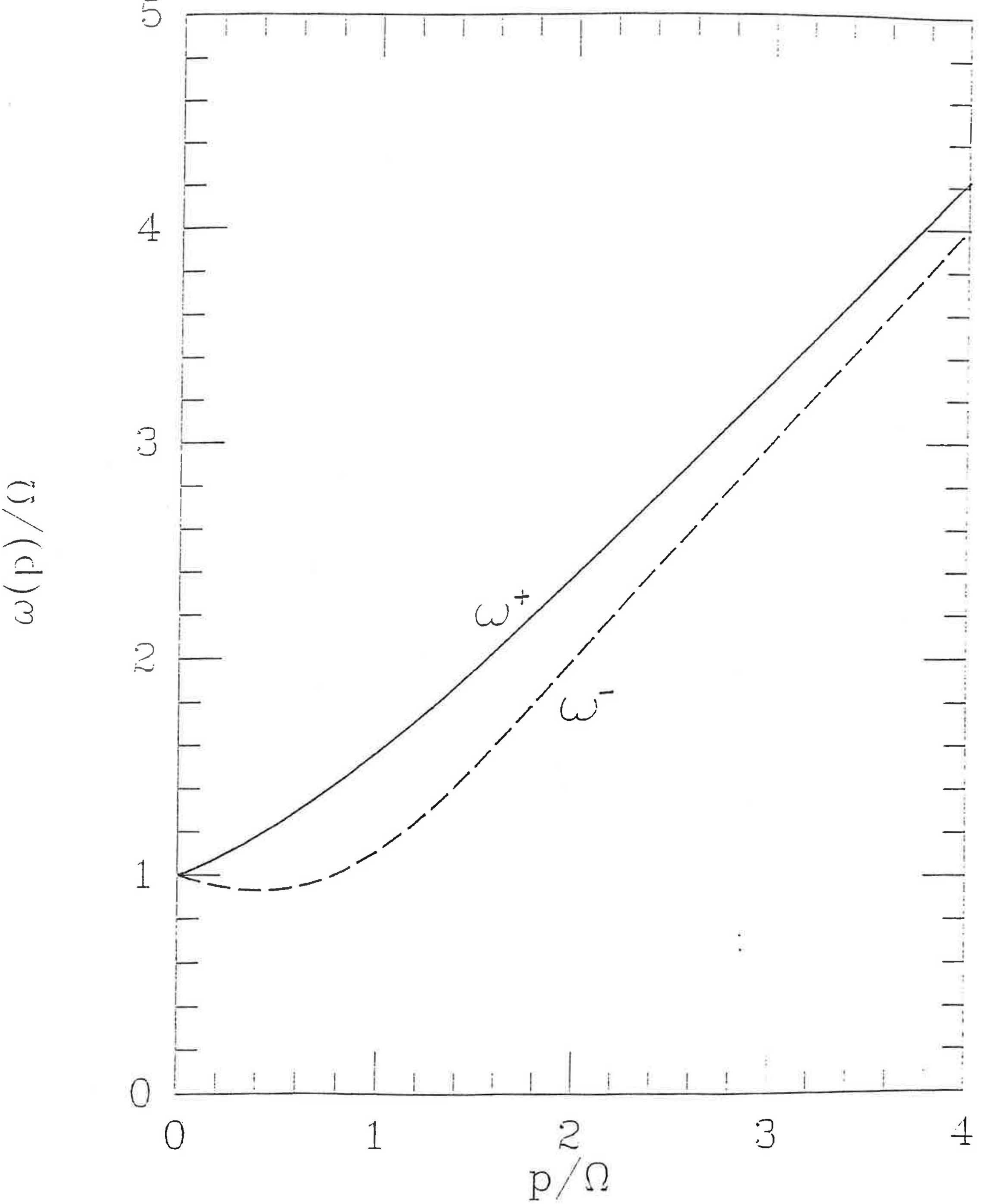


Figure 1

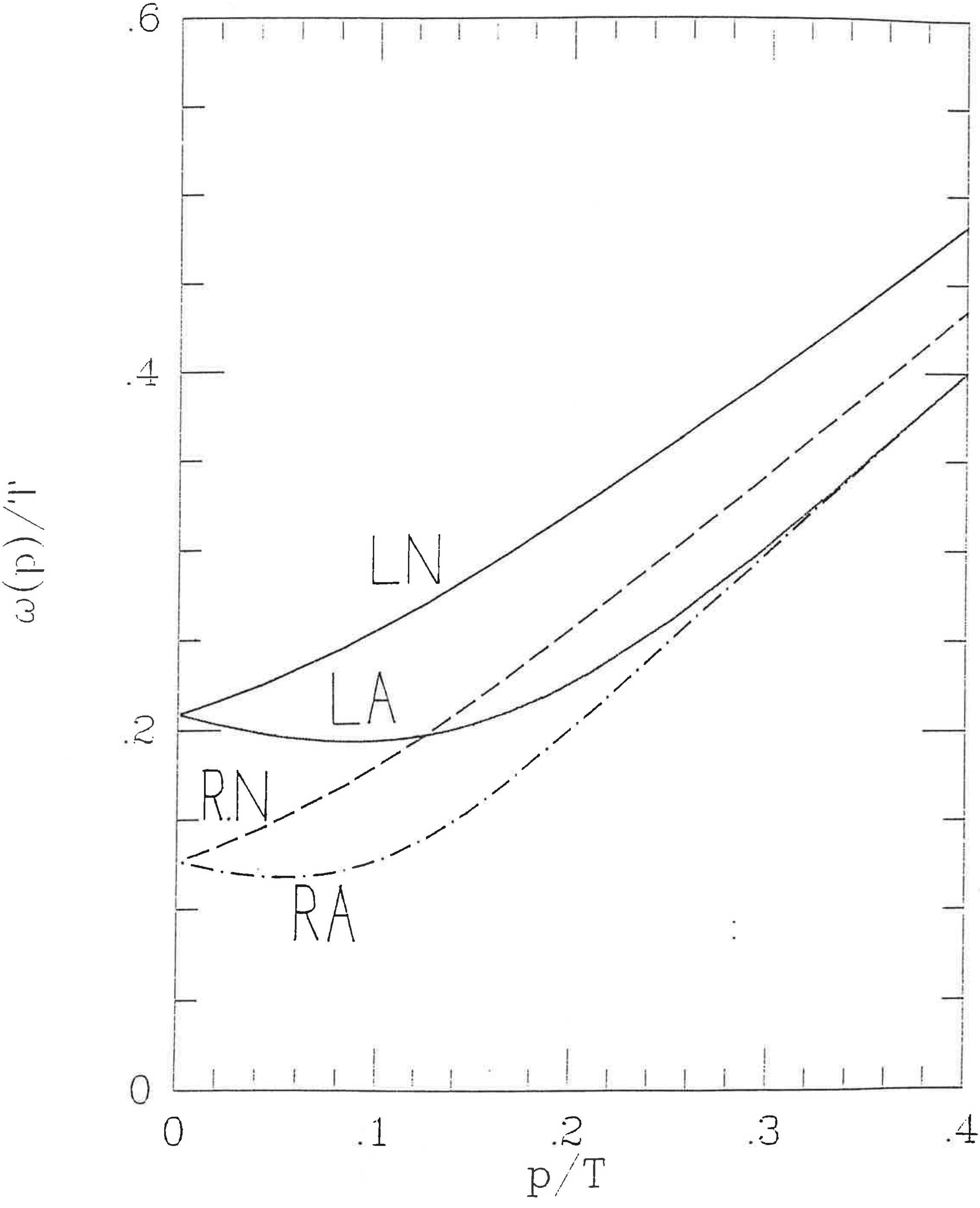


Figure 2

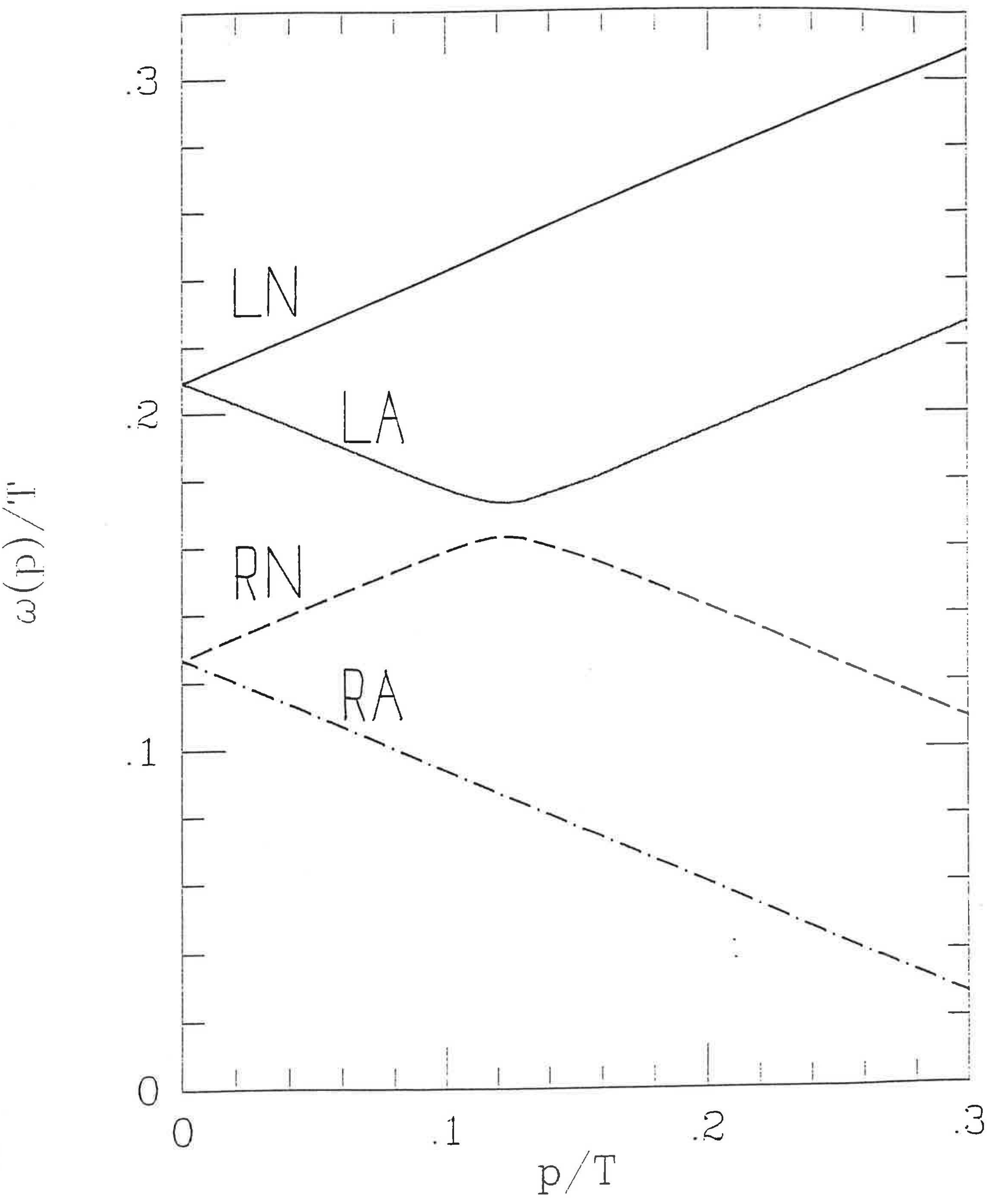


Figure 3

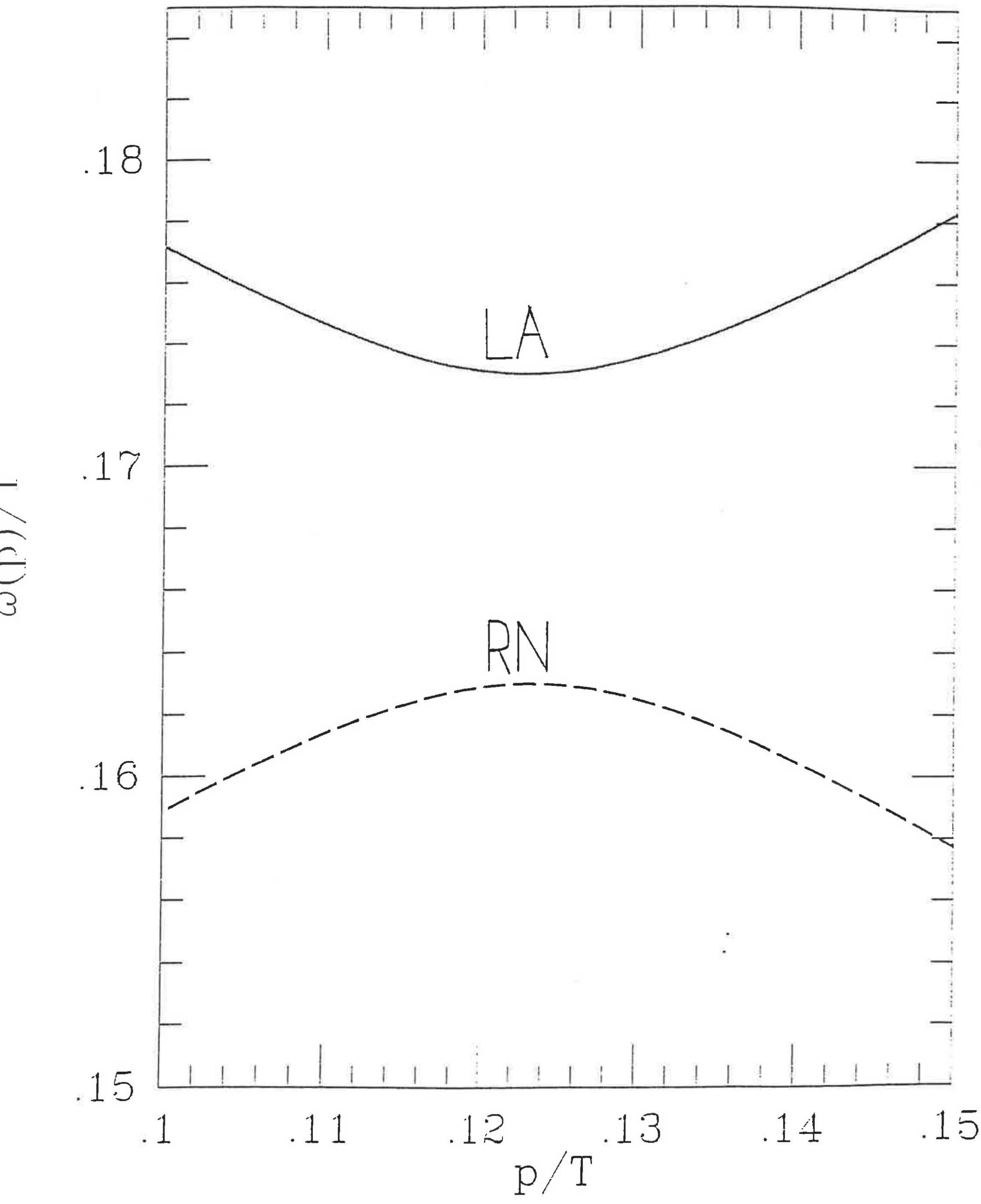


Figure 4

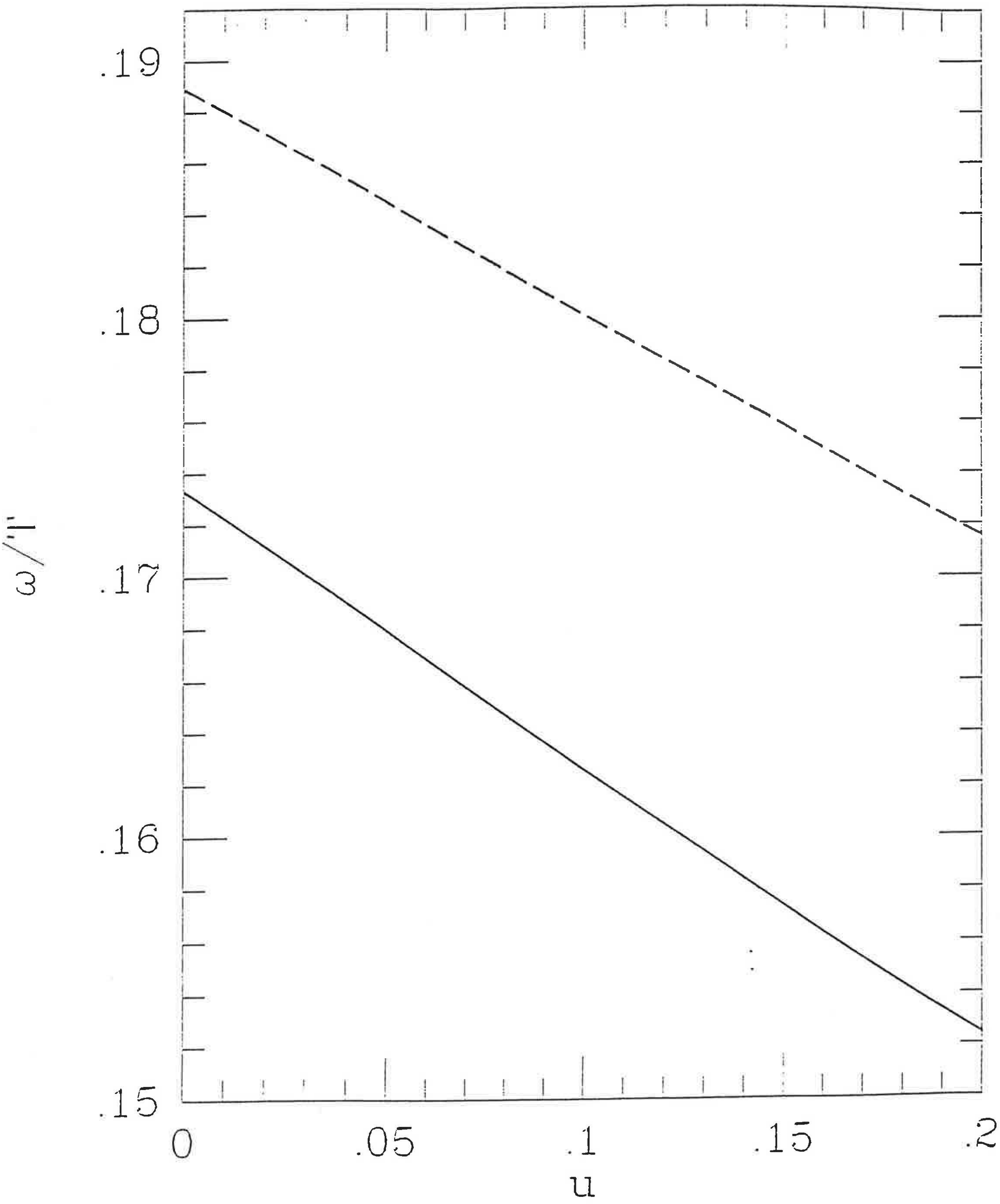


Figure 5